Buckling in polymer monolayers: Molecular-weight dependence

S. Srivastava and J. K. Basu[*]

Department of Physics, Indian Institute of Science, Bangalore 560 012, India
(Received 20 November 2008; revised manuscript received 10 February 2009; published 17 April 2009)

We present systematic investigations of buckling in Langmuir monolayers of polyvinyl acetate formed at the air-water interface. On compression the polymer monolayers are converted to a continuous membrane with a thickness of $\sim 2-3$ nm of well-defined periodicity, λ_b. Above a certain surface concentration the membrane undergoes a morphological transition buckling, leading to the formation of striped patterns. The periodicity seems to depend on molecular weight as per the predictions of the gravity-bending buckling formalism of Milner *et al.* for fluidlike films on water. However anomalously low values of bending rigidity and Young's modulus are obtained using this formalism. Hence we have considered an alternative model of buckling-based solidlike films on viscoelastic substrates. The values of bending rigidity and Young's modulus obtained by this method, although lower than expected, are closer to the bulk values. Remarkably, no buckling is found to occur above a certain molecular weight. We have tried to explain the observed molecular-weight dependence in terms of the variation in isothermal compressive modulus of the monolayers with surface concentration as well as provided possible explanations for the obtained low values of mechanical properties similar to that observed for ultrathin polymer films.

I. INTRODUCTION

Amphiphilic monolayers are known to form stable Langmuir monolayers at the air-water interface and can sustain fairly high surface pressure, Π [1,2]. However, on compression beyond a certain concentration these monolayers are known to become unstable to a collapse transition, usually accompanied by the formation of either multilayer islands on the surface or dissolution in subphase or both [1–5]. Under certain conditions this collapse transition is preceded by a mechanical instability called the buckling that leads to formation of regular striped pattern being determined by the mechanical properties of the monolayers [6–12]. Buckling or wrinkling has also been predicted and observed in thin elastic membranes on elastic substrates [13–18]. It has been shown that wrinkling stability occurs at a characteristic wave vector determined by the ratios of the stiffness of the substrate and the bending rigidity of the film [6–8,12,19]. These predictions have been found to hold for films on soft elastic substrate [5,12,19] as well as for monolayers on viscoelastic substrate [15,20] such as water, indicating the remarkably wide range of systems in which this phenomenon seems to be observed. However the treatment of buckling of a solidlike film on a viscous or viscoelastic substrate [20,21] is slightly different from that of either a fluid film on a viscous substrate [6] or a solid film on a solid substrate. Specifically the buckling wavelength scales with the ratio of bending rigidity and compressive stress than bending rigidity and substrate stiffness. The phenomena of buckling has also been incorporated as a technology for thin-film morphology whereby mechanical properties of their film on elastic substrate can be evaluated using the observations of their buckled patterns under compression or extension [22,23]. In certain cases buckling is detrimental for applicability of a particular material, and it has been shown recently [24] that incorporation of nanoparticles in polymer films can prevent buckling of such films. This also points to the role of local mechanical properties in determining buckling, something which has not yet been taken into account in the theoretical models. Although significant amount of work has been performed on buckling in thin films [11–13,16–19], very little work [6–9] has been done on Langmuir monolayers. Polymer Langmuir monolayers are ideal systems to study the role of monolayer mechanical properties on the buckling transition and its characteristic features. Variation in molecular weight is a very convenient way to change the intrinsic mechanical properties of the monolayers without changing the chemical nature or the monolayer substrate interaction and to study its effect on buckling in particular and morphological transitions in general on polymer Langmuir monolayers. Milner *et al.* [6] predicted that for polymeric monolayer the buckling wave vector, q_b, is expected to scale as

$$q_b = \left(\frac{K}{B}\right)^{1/4}. \tag{1}$$

The corresponding buckling periodicity can therefore be written as

$$\lambda_b = 2\pi\left(\frac{B}{K}\right)^{1/4}. \tag{2}$$

Here B is the bending rigidity of the monolayer and $K = \Delta\rho_m g$ where $\Delta\rho_m$ is the mass density difference between the air and the subphase (water) and g is the gravitational acceleration. Using an estimate of $B \sim N^{18/11}$ from scaling relations [25], one obtains the relation for variation in λ_b with N as

$$\lambda_b \sim N^{9/22}, \tag{3}$$

where N is the polymerization index. Here we have performed a systematic investigation of buckling transitions on

*basu@physics.iisc.ernet.in

Langmuir monolayers of polyvinyl acetate (PVAc) of three molecular weights (62 K, 246 K, and 361 K) formed at the air-water interface. Formation of buckled patterns with well-defined periodicity, λ_b, was confirmed through atomic force microscopy (AFM) on monolayers transferred onto solid substrates from air-water interface. We find that above a certain surface concentration of polymer, the monolayers form a very regular striped buckling/wrinkling pattern for 62 K and 246 K PVAc but surprisingly shows no buckling for the 361 K PVAc. The variation in λ_b with N seems to follow Eq. (3) approximately. However the obtained values of bending rigidity are anomalously low. An alternative explanation for the observed buckling has been provided in terms of a model of a solidlike layer on a viscoelastic substrate under compressive stress [20,21].

In Sec. II we discuss in detail the various experimental methods for the preparation and characterization of the PVAc monolayer including Langmuir-Blodgett techniques, x-ray reflectivity, and atomic force microscopy. PVAc monolayers of different molecular weight were prepared by Langmuir-Blodgett technique. The estimates of the monolayer thickness and the densities were obtained by detailed analysis of the x-ray reflectivity data using the Parratt formalism [26–28]. Atomic force microscopy was used to study the surface morphology of the transferred monolayers. Section III describes in detail the evolution of the buckling pattern with concentration and their comparison as a function of molecular weight which very closely follows the predicted scaling relations [6,25], except for the highest molecular weight of polymer. Finally in Sec. IV we provide our conclusions and outlook on the observed surface morphological features.

II. EXPERIMENTAL METHODS

A. Langmuir monolayers

It has been shown in many experiments in recent years [6–8] that Langmuir monolayers are the best system to perform very controlled measurements in two dimensions. The present set of experiments are based on Langmuir monolayers of PVAc of molecular weight 361 K ($N=4191$), 246 K ($N=2856$), and 62 K ($N=720$). PVAc solution in chloroform of concentration 0.2 mg/ml was spread at the water surface in a Langmuir trough of area 142 cm^2 (KSV, Finland). After the solvent evaporation ($\sim$15 min), the surface concentration was varied by compressing the barrier at constant speed (3 mm/min) and the isotherms (Π vs Γ) were recorded. The surface pressure was measured using the Wilhelmy plate with sensitivity of $\sim$0.01 mN/m. PVAc monolayers were transferred on a silicon (Silicon Quest, USA) substrate at different surface concentrations using the modified Schaefer method for characterization of surface morphology. Before the transfer of the polymer monolayer, the substrates were cleaned with acetone two to three times to remove any surface contamination and then etched with Piranha solution (mixture of H_2O_2 and H_2SO_4 in ratio of 3:1) to make the substrate surface hydrophilic. The transfer of the Langmuir monolayers on the silicon substrates was done at a very slow speed (0.5 mm/min) to avoid any damage of the film morphology due to transfer.

B. X-ray reflectivity

X-ray reflectivity measurements were performed on transferred monolayers using a Bruker D-8 Discover diffractometer with Cu K_α (wavelength of $\lambda=1.54$ Å) radiation. The incident beam was defined using a cross-coupled Goebel mirror followed by a 0.4×10 mm^2 slits before the sample. The reflected beam was collected using a scintillation detector with appropriate collimating slits (1×10 mm^2) after the sample and before the detector. The data were recorded as a function of perpendicular momentum transfer $q_z (=\frac{4\pi}{\lambda}\sin\theta)$.

C. Atomic force microscopy

AFM (Veeco CP2) measurements were performed on the transferred PVAc monolayers at different surface concentrations using contact mode with silicon probes (Mikromasch) of radius $\sim$10 nm (spring constant of 0.3 N/m and resonance frequency of 21 kHz).

III. RESULTS AND DISCUSSIONS

The size of a polymer chain, R_g, scales with the polymerization index, N, [$R_g \sim N^\nu$ where ν depends on the dimensionality of the system and is given by $\nu=3/(d+2)$, where d is the dimensionality of the system]. For a two-dimensional (2D) polymer chain under good solvent condition $\nu=3/4$. Scaling prediction [29,30] of the variation in osmotic pressure Π with Γ in the semidilute regime gives

$$\Pi \sim \Gamma^y, \quad y=\nu d/(\nu d-1), \qquad (4)$$

where ν is the Flory exponent, the value of which determines the interface condition for the polymer chain. In Fig. 1 we have shown the isotherms for PVAc monolayers of all the three molecular weights (361 K, 246 K, and 62 K). An extended linear region in the respective Π-Γ isotherms can be seen, from which the value of y has been evaluated using Eq. (4). This value turns out to be 2.90 ± 0.03, from which the exponent ν has been estimated to be $\sim$0.76. This value is remarkably close to the scaling prediction for 2D polymers in good solvent. At higher concentrations corresponding to the semidilute region, there is a clear change in slope in the isotherms at $\Gamma \sim \Gamma^{**}$. This marks the crossover from the semidilute to the concentrated phase and to possible changes in mechanical properties of the monolayer. The value of Γ^{**} is seen to vary slightly with molecular weight and varies between 0.8 and 1.0 mg/m^2. We have performed AFM imaging on transferred monolayers to study the morphological transitions across Γ^{**}, associated with this change in Π-Γ isotherms, the details of which have been discussed below. In Fig. 2 we present AFM images of the monolayers for PVAc 62 K at two surface concentrations Γ_h (1.5 mg/m^2) and Γ_l (1.1 mg/m^2). It is clear that at low concentration the morphology is almost flat while at the high concentration clear periodic striped pattern appears. The features seen in the image are typical of the transferred monolayers, and we have verified this by collecting images from different regions of
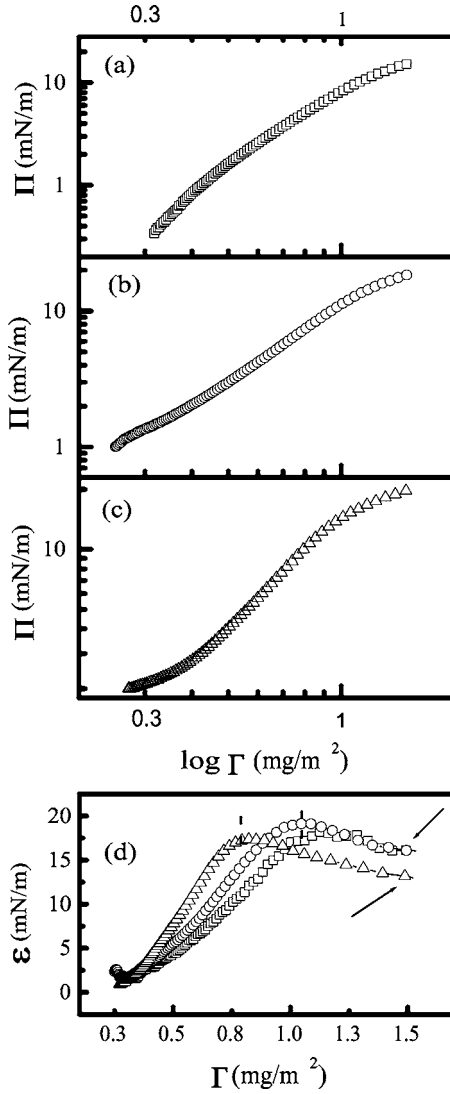
FIG. 1. Pressure Π vs surface concentration Γ for PVAc monolayers of molecular weight (a) 62 K (b) 246 K, and (c) 361 K. (d) The isothermal compressive modulus $\epsilon = \Gamma \left(\frac{\partial \Pi}{\partial \Gamma} \right)_T$ vs Γ for all the three molecular weights 62 K ($\square$), 246 K ($\bigcirc$), and 361 K ($\triangle$), respectively, of PVAc. The vertical dashed line alongside the data indicates the crossover concentration, Γ^{**}, for the respective molecular weights. Arrows indicate the concentration at which the films were transferred.

the sample. To obtain information on the periodicity of the buckled pattern, λ_b, we have taken the mean value from several such line profiles across the image. For 62 K PVAc transferred at Γ_h we find $\lambda_b \sim 130 \pm 10$ nm. On the other hand for the monolayers transferred at lower density, Γ_l, we find a completely flat surface morphology, indicating a clear lack of buckling or any other morphological transitions. Let us now compare similar AFM data on PVAc 246 K monolayers. As shown in Fig. 3, behavior similar to 62 K is found. At low surface concentration, Γ_l, the transferred monolayers are fairly smooth while at high concentration, Γ_h, the regular buckling pattern appears, indicating the presence of a critical surface concentration above which buckling sets in. The buckling periodicity, λ_b, in this turns out to be
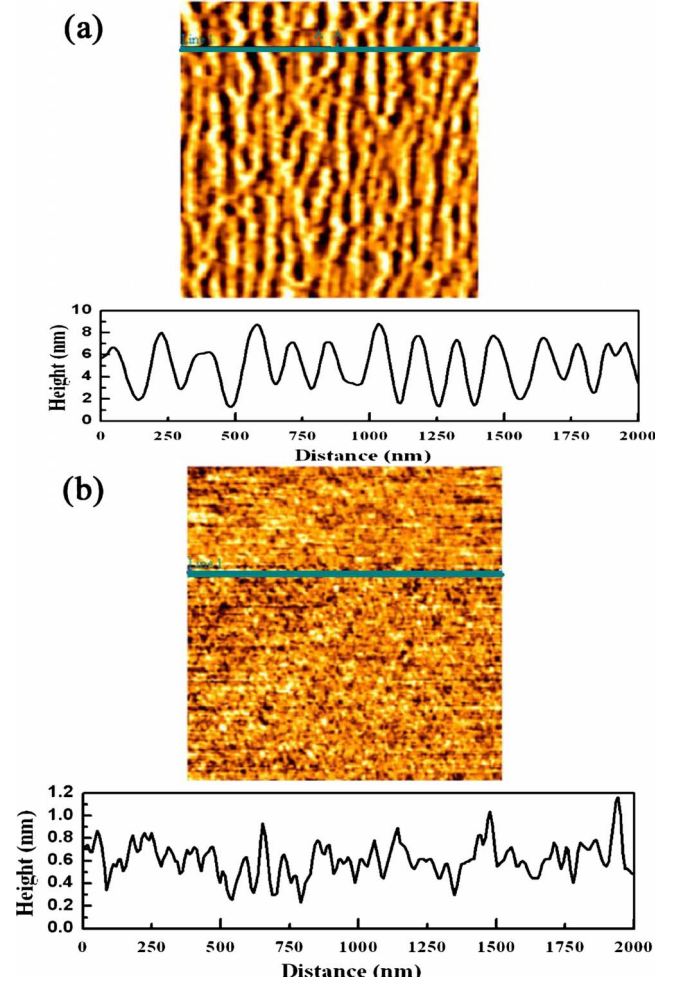

FIG. 2. (Color online) AFM images of the PVAc monolayer (62 K) on silicon substrate transferred using the modified Langmuir-Schaefer method at different Γ: (a) 1.5 mg/m^2 and (b) 1.1 mg/m^2. The height variation along the lines indicated on the images is shown below each image. The buckling period λ_b at Γ_h was calculated from the periodicity in the line profile as shown in (a).

$\sim 210 \pm 20$ nm. The buckling periodicity, λ_b, clearly depends on the molecular weight of PVAc. In Fig. 4 we show the power spectral density (PSD) extracted from fast Fourier transform (FFT) of the AFM images as shown in Figs. 2 and 3. The maxima in the respective PSD for 62 K and 246 K PVAc correspond to the respective q_b. For 62 K PVAc transferred at Γ_h we find $q_b \sim (4.8 \pm 0.4) \times 10^{-3}$ Å^{-1}, and for 246 K monolayer it varies from $(3.2 \pm 0.3) \times 10^{-3}$ Å^{-1}. Using Eqs. (1) and (3) we obtain

$$\frac{(q_b)_{62 \text{ K}}}{(q_b)_{246 \text{ K}}} \sim \left(\frac{N_{246 \text{ K}}}{N_{62 \text{ K}}} \right)^x \sim (3.97)^x. \qquad (5)$$

Using the respective values of q_b for 246 K and 62 K from Fig. 4 we obtain $x = 0.30$. The obtained value of x is also reasonably close to scaling predictions [Eq. (3)], thus suggesting that buckling in our systems could be determined by gravity and bending rigidity. Using *in situ* grazing inci-
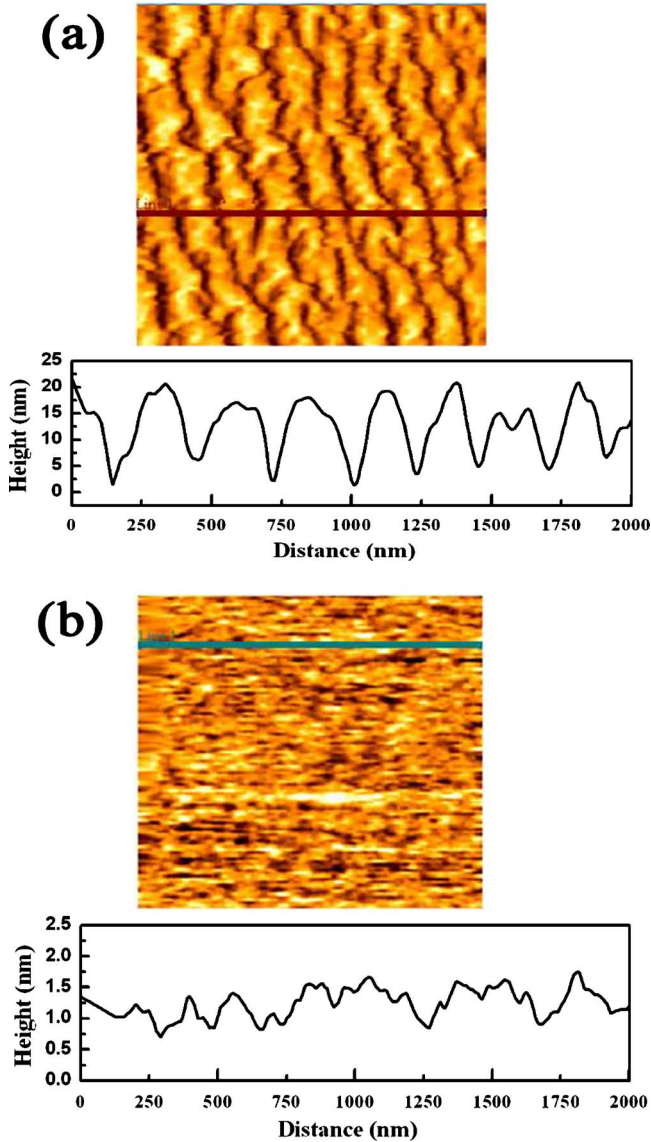
(a)

(b)

FIG. 3. (Color online) AFM images of the PVAc monolayer (246 K) on silicon substrate transferred using the modified Langmuir-Schaefer method at different Γ: (a) 1.5 mg/m^2 and (b) 1.1 mg/m^2. The height variation along the lines indicated on the images is shown below each image. The buckling period λ_b at Γ_h was calculated from the periodicity in the line profile as shown in (a).

dence small-angle x-ray scattering (GISAXS) measurements, reported in a separate communication [31] on 246 K PVAc monolayers, we have verified that the buckling periodicity on water and on silicon substrate is the same, clearly indicating that the observed features on monolayers after the transfer to solid substrates are a true representation of features already formed on water surface and show no major morphological rearrangements after transfer. Remarkably we find that for the monolayers of 361 K PVAc no buckling seems to occur. This is clearly evident from the AFM images of transferred monolayers in Fig. 5. At low concentration the transferred monolayers appear to be quite smooth similar to what was observed for the 246 K and the 62 K monolayers at similar surface concentrations. The high-density monolayer shows
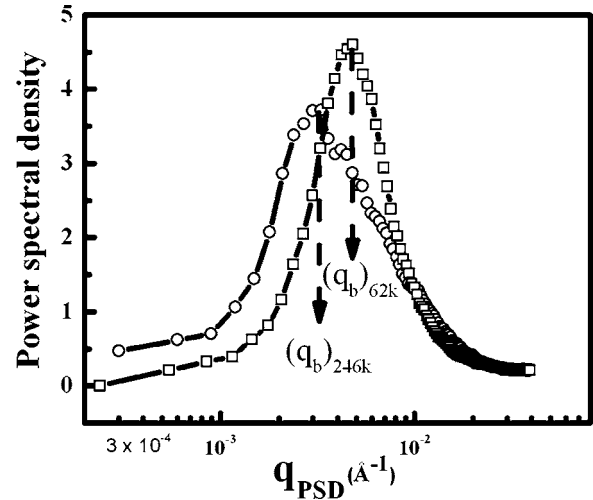

FIG. 4. PSD extracted from AFM image at Γ_h for PVAc monolayer of molecular weight 62 K ($\square$) and 246 K ($\bigcirc$), respectively. The maxima in the PSD correspond to the wave vector, q_b, as defined in Eq. (1).

structural inhomogeneities but no buckling. The scaling predictions do not provide any restriction on the applicability of the theory for certain molecular weight of polymers. Is it possible that some other factors are responsible for the observed buckling and especially the molecular-weight dependence? Langmuir monolayers are known to undergo morphological transformations such as multilayer formation or collapse at high concentrations [3–5]. Is it possible that such morphological transformations are responsible for the observed buckling?

Since AFM only provides information on surface topography, we have performed x-ray reflectivity measurements on the transferred monolayers to determine the thickness, electron density, and related parameters to rule out other possible reasons for the observed morphological transformations such as bilayer or multilayer formation. The fits to the respective reflectivity data were performed using a multilayer model based on the Parratt formalism [26–28] and are found to give excellent fits to all the data. The obtained electron-density profiles have also been shown for the respective data. Comparing the obtained density profiles for 62 K PVAc monolayers transferred at Γ_l and Γ_h, as shown in Fig. 6(b), we find that in the low-density phase the PVAc layer has a thickness of 16 Å and density of $0.15e/\text{Å}^3$ and that in the high-density phase it has a marginally higher thickness of 18 Å and electron density of $0.19e/\text{Å}^3$. It is clear that bilayer formation or major morphological transformation is not driving the observed morphology for this PVAc system. Similarly, the PVAc monolayer of 246 K transferred at Γ_h and Γ_l reveals thicknesses of 14 and 17 Å with densities 0.28 and $0.2e/\text{Å}^3$, respectively, as indicated in Fig. 7(b). The monolayer of PVAc for molecular weight 361 K has a thickness of 14 Å and density of $0.15e/\text{Å}^3$ at Γ_l and thickness of 35 Å and density $0.12e/\text{Å}^3$ at Γ_h [Fig. 8(b)]. The analysis of the reflectivity data for 361 K monolayers at Γ_h does seem to indicate significant change in thickness as compared to thickness at Γ_l. However it might be noted that reflectivity from such highly rough and inhomogeneous layers makes it difficult for
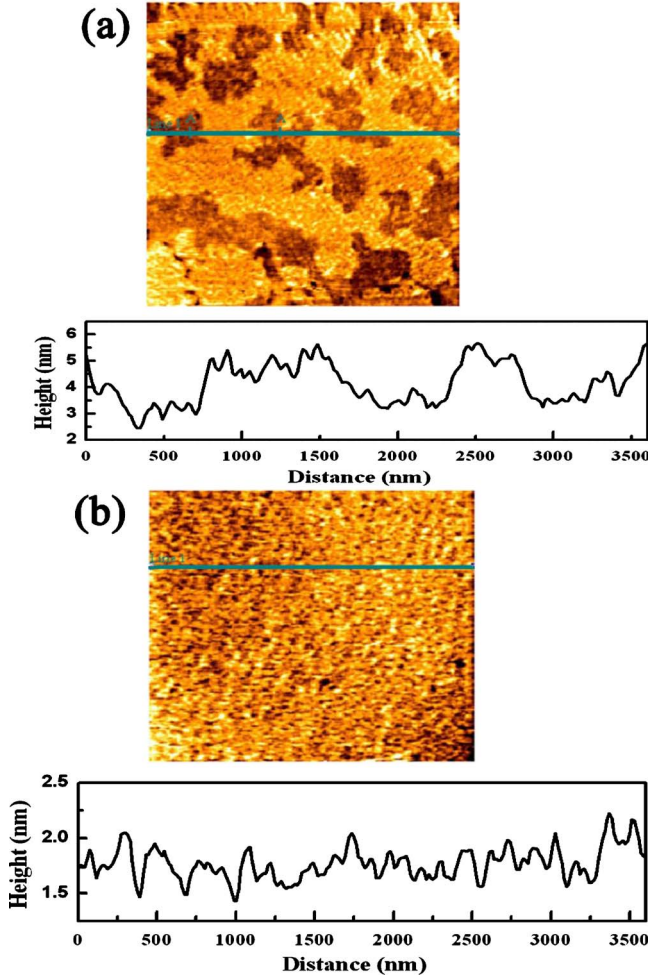
FIG. 5. (Color online) AFM images of the PVAc monolayer (361 K) on silicon substrate transferred using the modified Langmuir-Schaefer method at different Γ: (a) 1.5 mg/m^2 and (b) 1.1 mg/m^2. The height variation along the lines indicated on the images is shown below each image.

proper interpretation of results. It is also unlikely that there is a buckling transition taking place in 361 K PVAc monolayer between Γ_l and Γ_h which is followed by the collapse of the monolayer in such a narrow range of surface concentration ($\Gamma_l < \Gamma < \Gamma_h$). Recent *in situ* GISAXS measurements confirm this.

Clearly, the gravity-bending buckling does not seem to be able to explain the observed buckling phenomena, and there does not seem to be any other morphological transformations underlying the buckling we observe for the PVAc monolayers. We, therefore, consider an alternative model for buckling of these films based on the work of Huang and Suo [21]. The buckling periodicity λ_b scales as

$$\lambda_b = \sqrt{\frac{B}{\sigma h}}. \tag{6}$$

Here σ is the in-plane compressive stress and h is the thickness of the solid film. We estimate σ using the relation $\sigma_h \sim \frac{\epsilon_h \Delta \eta}{L} \sim 6$ kPa for 62 K and 246 K PVAc monolayers.
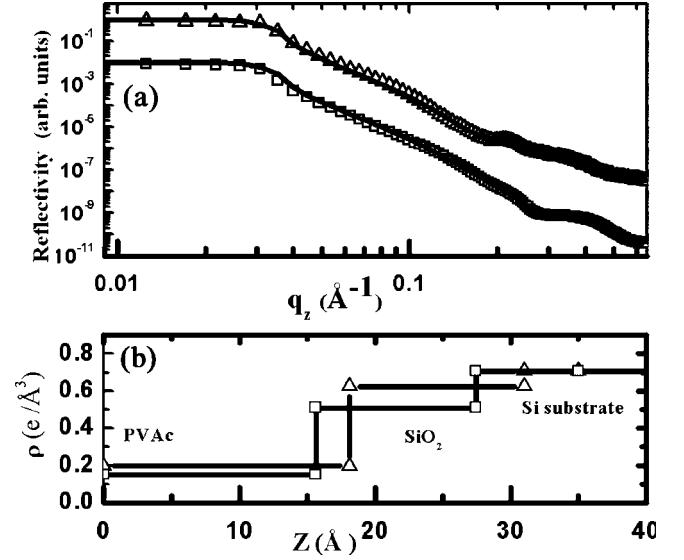

FIG. 6. Reflectivity data for PVAc monolayer of molecular weight 62 K (a) at Γ_h ($\triangle$) and at Γ_l ($\square$), respectively. The reflectivity data at Γ_l have been rescaled vertically for clarity. (b) Electron density, ρ, vs depth from the film surface, Z, extracted from the fits to the respective data.

Here $\Delta \eta$ is the compressive strain on the monolayer, ϵ is the compression modulus, and L corresponds to the Wilhelmy plate dimension. Using the obtained values of σ, the estimates of h from the reflectivity measurements and the observed buckling period, λ_b, in Eq. (6), we find that $B_{246\ K} \sim 0.10 K_B T$ and $B_{62\ K} \sim 0.05 K_B T$. Further, B can be related to Young's modulus E through the relation [6,8]

$$E = \frac{12\lambda^2 \sigma (1 - \nu^2)}{h^2}, \tag{7}$$

where ν is the Poisson ratio. Using Eqs. (6) and (7) we find $E_{62\ K} \sim 300$ kPa and $E_{246\ K} \sim 650$ kPa. Although these esti-
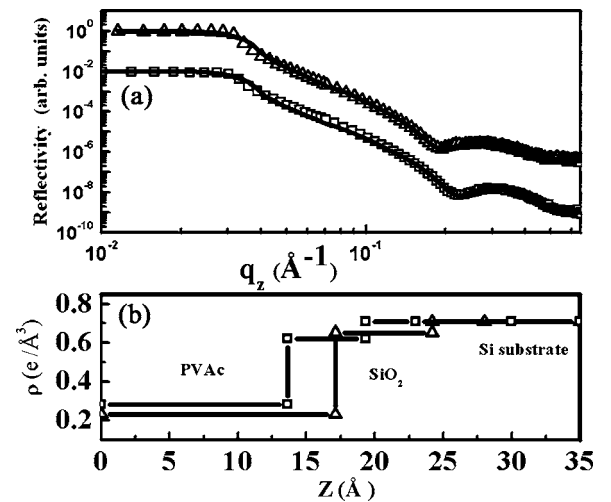

FIG. 7. Reflectivity data for PVAc monolayer of molecular weight 246 K (a) at Γ_h ($\triangle$) and at Γ_l ($\square$), respectively. The reflectivity data at Γ_l have been rescaled vertically for clarity. (b) Electron density, ρ, vs depth from the film surface, Z, extracted from the fits to the respective data.
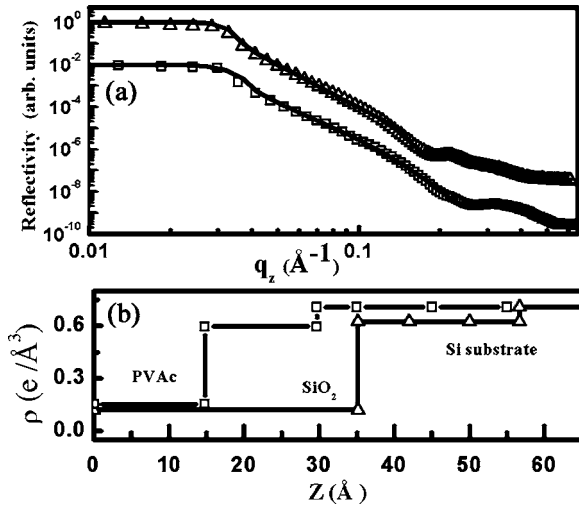
FIG. 8. Reflectivity data for PVAc monolayer of molecular weight 361 K (a) at Γ_h ($\triangle$) and at Γ_l ($\square$), respectively. The reflectivity data at Γ_l have been rescaled vertically for clarity. (b) Electron density, ρ, vs depth from the film surface, Z, extracted from the fits to the respective data.

mates are considerably lower than the bulk value of E for PVAc ($\sim$600 MPa) [32], they are much higher than what was obtained using the gravity-bending formalism of buckling [Eq. (1) or Eq. (2)]. However our estimates of B and E are based on the obtained values of σ measured using the Wilhelmy plate. These are expected to be on the lower side as it is known that the measurements of stress using Wilhelmy plate are likely to have error [12,33] when the monolayer becomes solidlike [34] at high surface concentrations. Thus the actual values of the modulus and the rigidity could be higher than the calculated values but are likely to be lower than the bulk values. It has also been observed earlier [35,36] that ultrathin polymer films or thin surface layers on bulk polymer have significantly lower mechanical properties than their bulk counterparts. What is the origin of the observed molecular-weight dependence of the buckling periodicity? Since the surface stress, σ, is independent of molecular weight and the monolayer thicknesses are also approximately the same for both molecular weights, at Γ_h, according to Eq. (7), the observed molecular-weight dependence of the buckling period can be related to the molecular-weight dependence of Young's modulus. The dependence of Young's modulus on molecular weight has also been observed earlier [37]. Why does the 361 K monolayer not buckle? To understand this let us see what drives buckling in these monolayer films. We generally observe that the film do not buckle below

Γ^{**}. It is known that PVAc monolayers enter a highly concentrated phase for $\Gamma > \Gamma^{**}$ and at the same time the compression modulus, ϵ, also decreases (Fig. 1). The resulting dense but compressible monolayer thus buckles under compressive stress. The change in ϵ as compared to $\epsilon_{\Gamma^{**}}$ is $\sim$15% for 62 K and 246 K at Γ_h. The change in modulus is considerably more for 361 K ($\sim$25%). The higher compressibility ($1/\epsilon$) might prevent the monolayer from buckling at intermediate compressive strain. At higher compressive strain the monolayer probably collapses, leading to the structure observed in Fig. 5. Although our proposed model does seem to explain the observed buckling phenomena in polyvinyl acetate monolayers of different molecular weights, we are performing more systematic measurements to understand the nature of micromechanical properties of the polymer monolayers which could be responsible for the reduction in mechanical properties as well as the molecular-weight dependence of buckling.

IV. CONCLUSIONS

In summary we have shown how buckling wavelength in monolayers of polyvinyl acetate depends on molecular weight. Surprisingly, for the highest molecular weight studied no buckling is observed for any surface concentration. Although scaling of the buckling wavelength, λ_b, with polymerization index seems to suggest presence of gravity-bending buckling, the obtained values of bending rigidity and hence Young's modulus of PVAc are anomalously low. Hence we have looked at an alternative scenario of buckling of a solidlike film on a viscous substrate rather than the fluid-on-fluid model implicit in the treatment of gravity-bending buckling. The values of B and E are much closer to the bulk values of PVAc but are still lower. This is consistent with the recent observation of reduced Young's modulus for ultrathin polymer films. However, we also do not rule out the necessity of introducing micromechanical effects to explain the observed behavior. Finally for 361 K PVAc we provide an explanation, based on reduced compression modulus, to the observed absence of buckling in such monolayers.

[1] G. L. J. Gaines, *Insoluble Monolayer at Liquid-Air Interfaces* (Wiley, New York, 1966).

[2] J. Meunier, D. Langevin, and N. Boccara, *Physics of Amphiphilic Layers* (Springer, Berlin, 1987).

[3] P. G. Mussone, A. F. W. Ip, S. L. M. Schroeder, B. S. Murray, and A. F. Miller, Langmuir **23**, 3766 (2007).

[4] H. E. Ries, Nature (London) **281**, 287 (1979).

[5] W. T. S. Huck, Nature Mater. **4**, 271 (2005).

[6] S. T. Milner, J. F. Joanny, and P. Pincus, Europhys. Lett. **9**, 495 (1989).

[7] L. Bourdieu, J. Daillant, D. Chatenay, A. Braslau, and D. Colson, Phys. Rev. Lett. **72**, 1502 (1994).

[8] F. Dubreuil, P. Fontaine, M. Alba, J. Daillant, J. W. Mays, G. Zalczer, and P. Guenoun, Europhys. Lett. **70**, 176 (2005).

[9] M. K. Bera, M. K. Sanyal, S. Pal, J. Daillant, A. Datta, G. U. Kulkarni, D. Luzet, and O. Konovalov, Europhys. Lett. **78**, 56003 (2007).

[10] J. Huang, M. Juszkiewicz, W. H. de Jeu, E. Cerda, E. T. Emrick, N. Menon, and T. P. Russell, Science **317**, 650 (2007).

[11] P. Peyla, Eur. Phys. J. B **48**, 379 (2005).

[12] L. Pocivavsek, R. Dellsy, A. Kern, S. Johnson, B. H. Lin, K. Y. C. Lee, and E. Cerda, Science **320**, 912 (2008).

[13] E. Cerda and L. Mahadevan, Phys. Rev. Lett. **90**, 074302 (2003).

[14] A. Lobkovsky, S. Gentges, H. Li, D. Morse, and T. Witten, Science **270**, 1482 (1995).

[15] Q. Zhang and T. A. Witten, Phys. Rev. E **76**, 041608 (2007).

[16] J. Genzer and J. Groenewold, Soft Matter **2**, 310 (2006).

[17] H. Vandeparre and P. Damman, Phys. Rev. Lett. **101**, 124301 (2008).

[18] W. T. S. Huck, N. Bowden, P. Onck, T. Pardoen, J. W. Hutchinson, and G. M. Whitesides, Langmuir **16**, 3497 (2000).

[19] N. Bowden, S. Brittain, A. G. Evans, J. W. Hutchinson, and G. M. Whitesides, Nature (London) **393**, 146 (1998).

[20] R. Huang, J. Mech. Phys. Solids **53**, 63 (2005).

[21] R. Huang and Z. Suo, Thin Solid Films **429**, 273 (2003).

[22] C. M. Stafford, C. Harrison, K. L. Beers, A. Karim, E. J. Amis, M. R. VanLandingham, H. C. Kim, W. Volksen, R. D. Miller, and E. E. Simonyi, Nature Mater. **3**, 545 (2004).

[23] A. J. Nolte, M. F. Rubner, and R. E. Cohen, Macromolecules **38**, 5367 (2005).

[24] T. R. Hendricks and I. Lee, Nano Lett. **7**, 372 (2007).

[25] P. G. de Gennes and C. Taupin, J. Phys. Chem. **86**, 2294 (1982).

[26] L. G. Parratt, Phys. Rev. **95**, 359 (1954).

[27] J. K. Basu and M. K. Sanyal, Phys. Rev. Lett. **79**, 4617 (1997).

[28] J. K. Basu, S. Hazra, and M. K. Sanyal, Phys. Rev. Lett. **82**, 4675 (1999).

[29] M. Daoud, J. P. Cotton, B. Farnoux, G. Jannink, G. Sarma, H. Benoit, C. Duplessix, C. Picot, and P. G. de Gennes, Macromolecules **8**, 804 (1975).

[30] P. G. de Gennes, *Scaling Concepts in Polymer Physics* (Cornell University Press, Ithaca, NY, 1979).

[31] S. Srivastava, J. K. Basu, M. Sprung, and J. Wang, J. Chem. Phys. (to be published).

[32] J. Brandrup, E. H. Immergut, and E. A. Grulke, *Polymer Handbook*, 4th ed. (Wiley, New York, 1999), Vol. I.

[33] A. Saint-Jalmes, M. Assenheimer, and F. Gallet, J. Phys. Chem. B **102**, 5810 (1998).

[34] T. A. M. Ferenczi and P. Cicuta, J. Phys.: Condens. Matter **17**, S3445 (2005).

[35] C. M. Stafford, B. D. Vogt, C. Harrison, D. Julthongpiput, and R. Huang, Macromolecules **39**, 5095 (2006).

[36] V. V. Tsukruk, A. Sidorenko, V. V. Gorbunov, and S. A. Chizhik, Langmuir **17**, 6715 (2001).

[37] S. Luo, D. T. Grubb, and A. N. Netravali, Polymer **43**, 4159 (2002).